Eurasian Journal of Physics and Functional Materials

Volume 2 | Number 1

Article 1

Pages: 6 - 16

3-22-2018

Reactions 11B + 209Bi at energies above Coulomb barrier

N. A. Demekhina
Yerevan Physics Institute, AANSL ,Armenia

A. R. Balabekyan
Yerevan State University ,Armenia

Yu. E. Penionzhevich
Joint Institute for Nuclear Research ,Russian Federation

N. K. Skobelev
Joint Institute for Nuclear Research ,Russian Federation

S. M. Lukyanov
Nuclear Physics Institute ,Russian Federation

See next page for additional authors

Recommended Citation

Demekhina, N. A.; Balabekyan, A. R.; Penionzhevich, Yu. E.; Skobelev, N. K.; Lukyanov, S. M.; and Burjan, V. (2018) "Reactions 11B + 209Bi at energies above Coulomb barrier," *Eurasian Journal of Physics and Functional Materials*: Vol. 2: No. 1, Article 1.
DOI: https://doi.org/10.29317/ejpfm.2018020101

Reactions 11B + 209Bi at energies above Coulomb barrier

Authors

N. A. Demekhina, A. R. Balabekyan, Yu. E. Penionzhevich, N. K. Skobelev, S. M. Lukyanov, and V. Burjan

Eurasian Journal of Physics and Functional Materials
2018, **2**(1), 6-16

Reactions $^{11}B + ^{209}Bi$ at energies above Coulomb barrier

N. A. Demekhina*[,1], A. R. Balabekyan[2], Yu. E. Penionzhevich[3,4], N. K. Skobelev[3], S. M. Lukyanov[3], V. Burjan[5]

[1]*Yerevan Physics Institute, AANSL Yerevan, Armenia,*
[2]*Yerevan State University, Yerevan, Armenia,*
[3]*Joint Institute for Nuclear Research, Dubna, Russia,*
[4]*National Research Nuclear University ?EPhI? Moscow, Russia,*
[5]*Nuclear Physics Institute, Rez, Czech Republic*

**e-mail: dem_nina@yahoo.com*

DOI: **10.29317/ejpfm.2018020101**
Received: 25.01.2018

Experimental data on production of radioactive residuals in $^{11}B + ^{209}Bi$ reaction a above-barrier projectile energy of 145.6 MeV are presented. The measurements and identification of reaction products were made using the method of induced activity. The residual nuclei in $24 \leq A \leq 211$ mass range are considered as products of different interaction channels, occurring through evaporation at complete, incomplete fusion and the fission. The fragments in (60-160) atomic mass units range are regarded to the fission products and are confirmed with data from experiments with analogous fissile nuclei. The residual nuclei near target mass number can be presented as result of the different processes including emission of nucleons and light nuclei. Theoretical predictions within the frameworks of PACE-4 code simulation, allowing the predictions of formation, evaporation and fission of compound nuclei, were used for analyzing the measurement results. A substantial contribution to production of residual nuclei of the incomplete fusion and of additional mechanisms, proceeding at different impact parameters, were revealed at analysis of the experimental data.

Keywords: cross section, break-up, fusion and fission reactions.

Introduction

In previous low energy experiments [1-4] the complete fusion (CF) and particularly incomplete fusion (ICF) were considered as probable processes appearing in interactions at different impact parameters. In a number of papers [5-8] ICF was predicted to occur along with CF depending on the projectile energy and mass asymmetry in the entrance channel. It was shown that the fusion of a projectile with target (CF) occurs presumably at values of angular momentum lower than the critical one ($l \leq l_{crit}$). At the critical value of angular momentum [9-11] and relatively large impact parameter the centrifugal forces increase, giving rise to peripheral collisions and direct interactions. The break up processes started to play an essential role also. The fusion with different light nuclei is localized in successive l-windows and can appear as a sequence of captures of different fragment mass by the target nuclei. The fraction of ICF accompanied by capture of separated fragments of the projectile became more probable, that are accompanied by building-up of the distribution of residual masses. The participation of break-up process in the nucleus - nucleus interactions are widely studied last years because in these experiments the structure properties of interacting nuclei

are visually demonstrated. An understanding of the details of break-up and fusion processes may shed light on important questions pertaining to the isotope production in the universe also. Experimental studies with radioactive nuclei would be very informative in these cases, but in view of low beam intensity this kind the results of measurements are not always statistically provided. The reactions with weakly bound nuclei are also of interest because if one of colliding nuclei has sufficiently low binding energy, it can break into component parts. The weakly bound light elements give an opportunity of studying the interactions of this kind with good statistics. In the present experiment ^{11}B nuclei is assumed to be a weakly bound system with relatively low binding energy in comparison with the large incident projectile energy. The process of ^{11}B nucleus break-up may be proceed via the different channels:

$$^{11}\mathrm{B} \rightarrow ^{7}\mathrm{Li} + ^{4}\mathrm{He}, \qquad Q = -8.665 \ \ MeV, \tag{1}$$

$$^{11}\mathrm{B} \rightarrow ^{8}\mathrm{Be} + ^{3}\mathrm{H}, \qquad Q = -11.224 \ \ MeV, \tag{2}$$

$$^{11}\mathrm{B} \rightarrow ^{4}\mathrm{He} + ^{4}\mathrm{He}, \qquad Q = -11.132 \ \ MeV, \tag{3}$$

The total cross section of reaction is presented usually as a sum of (CF+ICF) and the decrement of CF probability corresponds to the contribution of ICF. The reaction channel via ICF is usually considered as a two step process: the break- up of projectile in the vicinity of the target and fusion of the projectile part with the target nucleus. This process is being discussed mainly above the Coulomb barrier for incident beam energies ≥ 5 MeV and is characterized by the transfer of only a part of the projectile energy and momentum to the target nucleus. The measurements of reaction yields at different energies below and above the fusion barrier permit the checking of theoretically predicted correlation of different processes in the energy dependence and of the properties of participating nuclei. Previously it was shown [2,3] that in reactions induced by weakly bound light nuclei the cross section of CF was suppressed at above?arrier energies in comparison with the prediction of single barrier penetration and the coupled channel models. At high energies and with increasing impact parameter the different processes take place that are accompanied by projectile break-up. In the yields of ICF the missing cross sections due to many possible parts are found. Additionally the pre-equilibrium emission of particles and light nuclei is followed by an excitation energy decreasing and by a changing of residual nuclei composition. In earlier works at energies near and above the barrier the total fusion was considered mainly as developing via xn-, pxn- and αxn -evaporation channels and fission processes [2, 3]. At high energy the extension of the interaction channels and the addition of the different reaction products make the picture more complicate. The knowledge of the total composition of individual cross sections permits a detailed analysis of experimental data and sheds light on the role of different interaction mechanisms. In experiments using the activation methods the radioactive residual nuclei were measured as yields of definite channel reaction however the existence of the consistent chains of radioactive decays bring to mixing of the product yields. On the other side at

high energy the products of different interaction channels are located in the same mass region that creates difficulties in understanding of a reaction mechanism and testing of model predictions.

In reaction (^{11}B+^{209}Bi) CF leads to the production of ^{220}Ra compound nucleus and as a results of ICF via the (1)-(3) channels are formed ^{216}Rn, ^{213}At, ^{217}Fr, ^{212}Pb composite nuclei.

In the present work the yields of radioactive residual nuclei are related to $24 \leq A \leq 211$ amu. large mass region. The part of heavy residuals between compound nuclei and target masses (A_t) were considered mainly as products of CF and ICF. The activation method in experiments of this kind give information mainly about a completely or partly isobar chains, including a final or intermediate measurable isotopes in α - and $\beta^{\pm}$ - decay chains. The product mass range arranged approximately around $A_t/2$ as usually relates to the location of fission fragments. The fission cross section was determined based on analyzing the charge and mass distributions of fragments taking into account the regularities observed in previous experiments and obtained by using some empiric predictions. The fission process is usually considered as a direct indication of compound nucleus formation in CF. It is expected, that increasing transfer excitation energy and angular momentum followed by a diminution of the fission barrier and growth of the fission cross section. In this way the fission process is considered as a main indication on existence of the complete fusion.

In the present paper the experimental data were analyzed versus the reactions, producing similar compound nuclei, as the decay of compound systems were independent of the formation way. Substantially the obtained results were considered as compared with the fission and evaporation products from reactions with an analogous nuclear systems produced in (^{12}C+^{208}Pb), (^{13}C+^{207}Pb), (^{22}Ne+^{198}Pt), (^{12}C+^{209}Bi) reactions [12-16]. It was shown in [12], that the excitation functions of both the fission and (xn)-evaporation processes induced by ^{12}C and ^{11}B on ^{208}Pb and ^{209} Bi-targets were similar at energies ≤ 94 MeV. For comparison with theoretical predictions the calculations in the framework of PACE-4 code were used. The previously published data on (^{11}B+^{209}Bi) reaction were reanalyzed using calculated results.

Experimental methods

The irradiation with ^{11}B beam to 17nA intensity was made on ACCULINA-1 separator on U-400 accelerator (JINR, Dubna, Russia) using the standard stacked foil technique for reducing the incident energy in combination with high resolution gamma-spectroscopy. The mean value of projectile energy in the target was equal to 145.6 MeV. Bi target, 0.64 mg/sm^2 thickness was produced by evaporation on 0.54 mg/sm^2 Al-foil. The exposition on beam was continued during 12 hours. The induced activities were measured using high energy resolution HpGe ?etectors ($\sim$1.8 keV for 1330 keV line ^{60}Co) since the 3-rd hour after the irradiation up to two months. The energy and efficiency calibration of detectors was made by using a set of standard gamma sources (^{60}Co, ^{137}Cs, ^{154}Eu). The radioactive reaction products were identified based on spectroscopic characteristics from standard tabular data [17]. The cross sections of independent (I) and cumulative (C) reaction products are calculated using the general

expressions for activation analysis, allowing for contributions of radioactive precursors [18]. The errors of cross section values were estimated using the following factors: the statistical significance of experimental results ($\sim$ 2-5%), the accuracy in target thickness determination ($\sim$ 10%), accuracy of tabular value of nuclear constant ($\sim$ 3%) and errors in the detector efficiency determination with allowance for calculation of its energy dependence ($\sim$ 10%). The obtained cross sections for residual nuclei are presented in Table 1 and Table 2.

Table 1.
Cross section of fragments formed the reaction of 145.6 MeV ^{11}B-ions with ^{209}Bi. Independent cross sections are indicated by (I); others - cumulative (C).

Element	Type	Cross section, mb	Element	Type	Cross section, mb
^{7}Be	C	22.4±3.0	^{124}Sb	I	9.76±1.46
^{22}Na	C	6.3±1.2	^{126}Sb	C	2.83±0.42
^{24}Na	C	5.8±1.2	^{126}I	I	5.66±0.85
^{28}Mg	C	1.7±0.3	^{127}Sb	C	2.71±0.8
^{34m}Cl	I	0.9±0.2	^{130}I	I	2.15±0.32
^{38}S	I	0.5±0.06	^{131}Ba	C	2.23±0.32
^{38}Cl	I	0.3±0.03	^{133}I	C	0.90±0.14
^{39}Cl	C	0.3±0.03	^{135}I	C	0.94±0.18
^{41}Ar	C	0.2±0.04	^{136}Cs	I	1.94±0.27
^{42}K	C	0.15±0.03	^{140}Ba	C	1.80±0.26
$^{46(m+g)}$Sc	I	0.03±0.006	140La	I	0.52±0.10
^{54}Mn	I	0.05±0.01	^{141}La	C	2.02±0.30
^{57}Co	I	0.1±0.02	^{143}Ce	C	2.10±0.31
^{59}Fe	C	0.30±0.06	^{146}Gd	C	0.82±0.14
^{62}Zn	C	0.90±0.2	^{147}Nd	C	0.70±0.10
^{65}Zn	C	1.19±0.181	^{150}Pm	I	0.47±0.09
^{67}Ga	C	1.25±0.19	^{167}Tm	C	0.077±0.01
^{69}Ge	C	1.92±0.27	^{169}Lu	C	1.57±0.20
^{72}Zn	C	0.90±0.13	^{170}Hf	C	1.50±0.23
^{73}Se	C	0.65±0.08	^{171}Lu	C	16.0±2.4
76As	I	4.71±0.6	^{173}Hf	C	8.2±1.2
^{77}Ge	C	0.520±0.08	^{175}Hf	I	0.50±0.075
^{77}Br	C	0.90±0.013	^{175}Ta	C	3.70±0.5
^{82}Br	I	9.20±1.3	^{177}Ta	C	0.85±0.16
^{83}Rb	I	7.05±1.01	^{181}Re	C	10.30±1.5
^{83}Sr	C	0.73±0.1	^{182}Os	C	23.10±3.3
^{84}Rb	I	11.91±1.69	^{183}Os	C	6.50±0.92
^{86}Rb	I	16.150±2.4	^{183}Re	C	0.11±0.02
^{87g}Y	I	2.80±0.42	^{186}Ir	C	16.60±2.45
^{87m}Y	C	3.43±0.4	^{188}Pt	C	0.62±0.09
^{89}Zr	C	2.80±0.42	^{189}Pt	C	30.0±4.5
^{90m}Y	I	36.44±4.4	^{191}Pt	C	5.81±0.82
^{91}Sr	C	41.09±6.1	^{192}Au	C	13.95±2.43

Table 1. Continued.

Element	Type	Cross section, mb	Element	Type	Cross section, mb
^{91m}Y	I	8.30±1.2	^{193}Au	C	9.61±1.36
^{92}Sr	C	25.10±3.7	^{194}Au	I	24.63±3.6
^{92}Y	I	6.10±0.91	^{195}Au	I	1.44±0.21
^{93}Y	C	42.60±6.3	^{195}Hgg	I	28.5±4.2
^{95}Zr	C	36.55±4.7	^{195}Hgm	C	46.4±6.64
^{95g}Nb	I	3.70±0.5	^{196}Aug	I	0.42±0.06
^{95m}Nb	I	2.83±0.4	^{196}Aum	I	0.39±0.06
^{96}Nb	I	36.90±5.5	^{197}Hgg	I	37.4±5.4
^{97}Zr	C	42.52±7.5	^{198}Aug	I	0.37±0.051
^{97}Nb	I	22.12±3.3	^{198}Aum	I	0.11±0.015
^{99}Mo	C	44.12±6.60	^{198}Tl	C	50.0±7.5
^{99m}Tc	I	9.20±1.3	^{199}Tl	I	100.0±15
^{102m}Rh	I	14.22±2.1	^{200}Pb	C	85.2±12.44
^{103}Ru	C	58.12±8.9	^{201}Tl	I	160.3±24.1
^{105}Ru	C	66.06±9.61	^{201}Pb	C	58.4±8.7
^{105}Rh	I	18.40±2.74	^{202}Tl	I	3.2±0.43
^{110m}Ag	I	21.20±3.12	^{203}Pb	I	23.6±3.4
^{111m}Pd	I	33.23±3.32	^{203}Bi	C	68.7±10.3
^{111}Ag	I	9.25±0.93	^{204}Bi	I	75.0±7.5
^{112}Pd	C	48.11±7.5	^{204}Po	C	56.2±8.4
^{112}Ag	I	9.73±1.41	^{205}Bi	C	67.0±10.055
^{113}Ag	C	43.12±5.90	^{206}Bi	I	58.2±8.7
^{115m}Cd	C	30.84±4.58	^{206}Po	C	38.7±5.8
^{117g}Cd	C	9.80±1.43	^{207}Po	C	35.3±5.2
^{117m}Cd	C	12.53±1.85	^{209}At	C	26.2±3.9
^{117g}In	C	4.57±0.66	^{210}At	C I	54.6±8.1
^{117m}In	I	2.71±0.56	^{210}Rn	C	136.0±20.6
^{117m}Sn	I	1.1±0.2	^{211}Rn	C	63.0±9.3
^{120m}Sb	I	5.72±0.8			
^{122}Sb	I	11.34±1.63	-	-	-

Table 2.
Values of fission parameters obtained at fitting and calculations.

	Experiment	Calculation PACE-4
$\bar{A}$	104 ±1.6 amu	
FWHM	30.42±1.2 amu	
σ_f (mb)	1296.4±160.6	
σ_{tot} (mb)	2100±200	1910

Fission

In reaction (^{12}C+ ^{208}Pb) two asymmetric and one symmetric fission components were observed at the excitation energy E* ∼ 24 MeV [19]. The asymmetric fission shoulders disappeared practically at E* ∼ 53 MeV. In our experiment,

according to PACE-4 code calculations, the excitation energy and angular momentum are E* ~ 118 MeV and $l \leq 78\hbar$. These initial conditions suppose that the fission fragments are formed of a single symmetric component. The bell shaped distribution obtained in (60-160) atomic mass range (Figure 1) is considered as a binary mode of fission of ^{220}Ra compound nucleus.

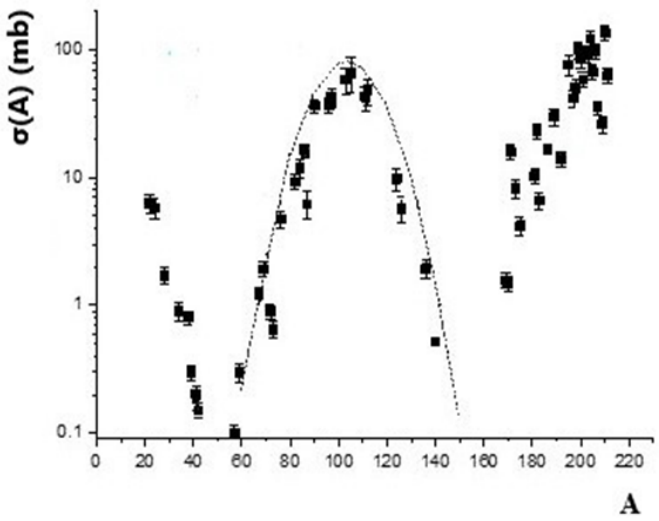

Figure 1. Cross sections for production of the residual nuclei from reaction (^{11}B +^{209} Bi). Dotted line – fission cross section (see text).

The fission cross section was calculated based generally on the assumption of Gaussian function form for the fragment charge and mass distributions [20, 21]. The cross section of independently produced fission fragments σ(A, Z) can be presented as Gaussian Z-distribution curve at given A-value:

$$\sigma(\mathrm{A,Z}) = \sigma(\mathrm{A})/[\mathrm{C}(2\pi)^{1/2}]\exp[-(\mathrm{Z\text{-}Z}_p)^2]\mathrm{C}^2), \quad (4)$$

where σ(A) is the total isobaric cross section for given A, Z_p is the most probable charge and C is the parameter of the distribution width. In order to uniquely specify the variables σ(A), Z_p and C one needs to measure at least three independent cross sections for each isobar. The spectroscopic analysis of induced activity is not generally provided with data on several isobars required for determination of necessary parameters. As in previous publications [20, 21], in the present work several assumptions on the basis of results of earlier measurements and the empiric applications were made. The first assumption relates to the slow dependence of the parameter of charge distribution widths (C) on the product charge number (Z) for the regions with close mass numbers. Another assumption is that the charge distributions of the fission fragments are similar for the closed mass number and the corresponding parameters are depended mainly on the nuclear composition of fragments. The cross sections of a particular isotopes (in experiments like this) can be independent or cumulative (partly or completely) due to the presence and the decay of precursors. The beta-feeding correction factors for the cumulative isobaric yield can be calculated once the centroid and width of the Gaussian are known. For obtaining the fitting parameters Z_p and σ_A the least-squares method was

employed. In this way the measured cross sections were adjusted successively to remove the precursor feeding (where necessary) and a set of independent cross sections were generated. The mass-yield distribution was constructed (Figure 1) using the calculated values of σ_A corresponding to the isobaric cross sections for a specific mass numbers. The total isobaric distribution was obtained by fitting the Gaussian form with certain values of the height - λ_A, mean mass number - $\bar{A}$ and width parameter - Γ_A:

$$\sigma_f = \lambda_A \exp(-(A - \bar{A})^2/\Gamma_A), \tag{5}$$

The fission cross section as obtained by summing all isobaric yields is equal to $\sim(1296.4 \pm 160)$ mb. The obtained experimental fission cross sections with data for ^{11}B + ^{209}Bi reaction [2], and data for (^{12}C+ ^{208}Pb) [13, 23] reaction are presented in Figure 2 along with the calculation results by PACE-4 code. The data in Figure 2 show that the fission cross section increases near the barrier and then slows down up to reaching a plateau. The fission cross section is usually regarded to the complete fusion process. At lower energies $\sim$75MeV [2] the contribution of incomplete fusion with ^{4}He and ^{7}Li ions produced via the break-up of ^{11}B was approximately estimated to be $\sim$1%. Similarly, the fraction of ICF -fission at $\sim$13MeV/nucleon can be estimated as being no more than several percent taking into account the break-up and fission probabilities [24, 25]. This value is within the accuracy of the present experiment. At high excitation energy and high angular momentum of the compound nucleus the decreasing of fission barrier leads to the prevalence of fission process. In a number of model predictions the ratio of fission cross section to the complete fusion cross section is assumed to be approximately equal to $\sim(0.7 \pm 0.1)$ and weakly depend on the type of projectile. The total reaction cross section as estimated for this value of ratio is (2100 ± 300) mb. For comparison, in the frameworks of PACE-4 code the fission cross section was calculated to be $\sim$1540 mb and the total cross section of reaction $\sim$1910 mb. If the decrease in fission cross section is treated as the contribution of incomplete fusion [2], then an approximate estimate of the suppression of complete fusion via fission gives 121.8 %. This value is not at variance with previously obtained complete fusion suppression effect ($\sim$7%) in (^{11}B+ ^{209}Bi) reaction at energy 75 MeV and can be considered as a consequence of ICF increasing with the energy of projectile.

At fitting of experimental data the values obtained for the centroid of mass distributions of fission fragments and for the width parameter were A=(104 ± 15) amu and C $\sim(12.9 \pm 20)$ amu (FWHM $\sim$30.2 amu) respectively. The mass number of fissioning nucleus was determined as 208 amu and the total number of nucleons emitted before fission $\sim$12 (including the pre- and post-fission neutrons). At lower energies of 73.4 MeV and 84.2 MeV [25] the centroids of mass distributions in reaction (^{12}C+ ^{209}Bi) were obtained to be 107.7 amu and 107 and FWHM $\sim$24.8 and 25.4 amu respectively. These data agree with our results, taking into account increasing of the neutron evaporation with excitation energy and following enlargement of the fissioning nuclei number. The maximum of isobaric curve landing approximately at Z $\sim$ 44 (Z $\sim$ 88 - for fissioning nucleus) is explained by the preferential neutron emission before the fission.

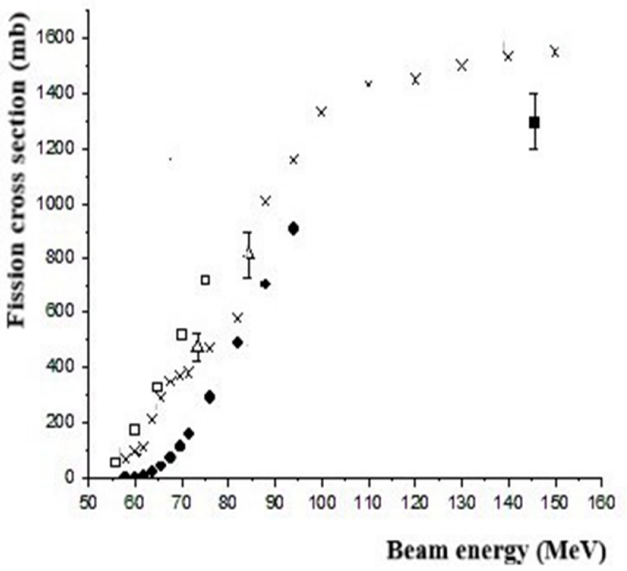

Figure 2. Fission cross section : □ - data [2]-reaction (^{11}B + ^{209}Bi), • - data [13] -reaction (^{12}C + ^{208}Pb), Δ - data [16]-reaction (^{12}C + ^{208}Pb), ■ - present work, × - PACE-4 code calculation - reaction (^{11}B + ^{209}Bi).

Heavy reaction products

A number of residual nuclei formed approximately in the mass range between the compound ^{220}Ra nucleus and target ($\Delta A \sim 20$) are considered as products of CF and ICF followed with emission of nucleons and light nuclei. As was pointed out above, the initial conditions of the reaction- the excitation energy and angular momentum predicted by PACE-4 calculations, suppose an essential role of ICF [13, 26] and decrease of CF, that are most probable at lower angular momenta. The composite nuclear states produced at high angular momentum preferentially undergo the fission decay. The presence of preequilibrium processes appears as the emission of neutrons, protons, α-particles and other fragments before statistical equilibration [28-30]. The heavy cluster emission from highly excited nuclear systems was considered in detail in [27] for $\Delta Z \leq 10$ charge loss processes. In addition, the inelastic scattering of projectile on the target surface may lead to low energy transfer followed with emission of several nucleons. At subsequent α- and β-decays of heavier precursors are populated a number of lighter nuclei. Usually, CF reaction channel is revealed through a sum of the decays including xn-, α xn-, pxn- emission from compound nucleus. In (^{22}Ne + ^{198}Pt)-reaction [14] these evaporation for the compound nucleus ^{220}Ra, excited up to (100-120) MeV, are measured in a mass spectrometer via the short lived α-active reaction products formed as a results of xn- evaporation. The obtained cross sections for ($p8n$-$p9n$)-reactions $\sim$1 mb, for ($p10n$-$p11n$)-reactions $\sim$2 mb and the same order of the cross sections of for emission of α-particles in ($\alpha\,10n$), ($\alpha\,11n$) reactions. The cross sections of Rn-isotopes formation proved to be significantly larger than those expected from α-decay of Ra parents, produced in xn?mission processes. CF yields were defined in [2, 14] by comparing the measured cross sections for (^{12,13}C+ ^{208,207}Pb) and (^{10,11}B+ ^{209}Bi) reactions with statistical model calculations of (^{30}Si+ ^{186}Wi) fusion at above-barrier energy. The compound nucleus in the last ^{216}Ra case was considered as CF and the projectile ^{30}Si was considered as a normal, strongly bound, noncluster struc-

ture nucleus. So, the statistical model describing the evaporation probability in (^{30}Si+ ^{186}Wi) reaction was used for reliable prediction of cross sections for similar processes in ^{10,11}B and ^{12,13}C induced reactions. The required extrapolation was made for a transfer from ^{216}Ra to ^{219,220}Ra compound nuclei and correction of the values of angular momentum and fission barrier. The calculated cross section for production of Ra isotopes through neutron evaporation from a compound nucleus is much smaller than the experimental values obtained for Rn yields assumed as products of α-decay of Ra. Nearly 80% of directly produced Fr and Rn isotopes was obtained to be due to ICF.

The method of induced gamma-activity in present work does not allow to obtain the yields short lived α-decaying Ra isotopes, populating Rn nuclei, which in its turn undergo via the α-decay and the consistent β^+ - conversion into Po, At isotopes. Fr-isotopes can be formed in ($px n$) reactions and can be transformed through the α-decay also to At isotopes. On the other side, ($\alpha x n$) channel in ICF leads to the creation of Rn isotopes and via successive α, β^+-decays to low lying elements. The reaction channels followed break up ^{11}B and incomplete fusion ^{7}Li and ^{4}He fragments are resulted to compound nuclei ^{216}Rn and ^{213}At and can participate in populating Rn, At, Po isotopes. A number of underlying elements can be formed via particles emission and radioactive decay processes. The experimental data of the present work give large yields of Rn, Po and At isotopes, that is indicative of aforementioned significant contribution of ICF. The production of Bi-isotopes can find out as an inelastic scattering leading to the transfer of insignificant excitation energy to the target nucleus and emission of small number of neutrons [31]. Due to such a mixing it turns impossible to extract separate interaction channel without prior chemical separation. The isobars with measurable spectroscopic characteristics may provide a partial or full summary effect. The mass distributions of such residuals give a complicated picture including all processes to occur.

Calculations in frames of PACE-4 code give the cross sections of evaporation products produced via neutrons, protons and α-particles evaporation using statistical model for reaction representation [32]. The calculation cross sections of the individual reaction products can? compare with experimental data directly because the measurements relates mainly to the cumulative yields.

For comparison the calculation results can be summed including the products of consecutive decay channels. We think that in this way one can obtain the estimates of CF contribution in the measurements data. In Figure 3 are presented the calculation and measurement results. The experimental data are seen to sufficiently exceed the calculation results and shifted to lower mass range. This excess may be due to the contribution of ICF. As was shown in [14], $\sim$80% part of Rn isotope cross sections can be attributed to increasing contribution of ICF processes. The displacement of distribution to lower masses can be explained as due to increased excitation energy and involvement of additional interaction channels. The high cross sections, observed for products near the target mass number, can be explained by the contribution of inelastic scattering and transfer processes following small number transmission nucleons.

The independent cross sections of several isotopes in $160 \leq A \leq 190$ mass range (Au, Hg, Re) and residuals in $A \leq 50$ range seemingly result from binary processes with heavy fragment emission considered in detail in [27] for ion in-

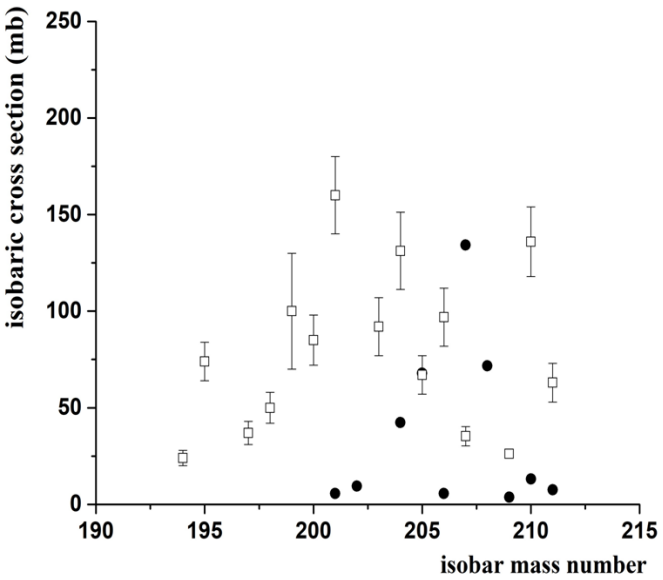

Figure 3. Heavy residual product- isobars from reaction (^{209}Bi + ^{11}B): □ - experimental data; • - PACE-4 calculation results at two near excitation energies, summed on the mass number.

duced reactions. The high probability for formation of ^{198m} Au and ^{196m} Au isomer states (12^{-}) may be an indication of high spin value of preceding intermediate composite nucleus. The transition of this kind appears more probable as the first fast step of the interaction with emission of the accompanying fragment. There are different opinions on the formation probability of an intermediate mass fragment: in [32-36] the fragment formation was ascribed to the coalescence of nucleons during the nucleon-nucleon interaction cascade started as soon as two nuclei come into contact; in [17] the authors developed a method for calculation of the probability of heavy fragment emission from excited nucleus with simultaneous evaporation of nucleons. The other probable way for formation of residuals of this kind can be the asymmetric decay of highly excited nuclei.

Conclusions

The study of (^{11} B+ ^{209} Bi) interaction at energy 145.6 MeV showed the mixing of different interaction channels occurring at the residuals distribution. The fission cross section of (1296.4 ± 190) mb obtained at analyzing the distribution of fission fragments proved lower than the model predictions using PACE-4 code (1540 mb). Assuming the fission process as the most probable channel of compound nuclei decay in CF at given energy, one can regard the decrease in fission cross section as an estimate of $(12 \pm 1.8)\%$ suppression of this CF channel. Characteristics of the charge and mass distributions of fission fragments well agree with data from reactions with similar fissioned nuclei under near energy conditions. The transfer of excitation energy to the compound nuclei became apparent in case of 12 emitted nucleons in the fission channel (including pre- and post-fission neutrons). The main part of heavy reaction products are created in ICF followed with evaporation of nucleons and a sequence of radioactive transformations. The yields of intermediate mass fragments and several heavy isotopes may be explained by supposing the contribution of possible asymmetric decay or emission of heavy fragments at high excitation energy.

Acknowledgments

Authors are grateful to the teams of the cyclotron U-400M and ACCULINA-1 separator for the beam quality during the course of bombardment run. Thanks are due also to G. S. Karapetyan for collaboration in this work.

The present work was performed with the support of RSF by grant No.17-12-01170.

References

[1] P.R. Gomes et al., Phys. Rev. C **84** (2011) 014615.
[2] N.K. Skobelev et. al., Phys. Part. Nucl. Lett. **10** (2013) 248.
[3] L.R. Gasques et al., Phys. Rev. C **79** (2009) 034605.
[4] P.P. Singh et al., Phys. Rev. C **77** (2008) 014607.
[5] H. Morgenstern et al., Phys. Rev. Lett. **52** (1984) 1104.
[6] A. Yadov et al., Phys. Rev. C **85** (2012) 034614.
[7] V.E. Viola et al., Phys.Rev.C and references there in **28** (1982) 178.
[8] A.A. Souzongui et al., Phys. Rev. C **53** (1996) 243.
[9] J. Wilczynski, Nucl. Phys. A **216** (1973) 386.
[10] T. Sikkeland, Phys. Rev. B **135** (1964) 669.
[11] R. Bass, Nucl. Phys. A **231** (1974) 45.
[12] H. Marshall Blann, Phys .Rev. **123** (1961) 1356.
[13] K. Kalita, Jour. Phys G. **38** (2011) 095104.
[14] A.N. Andreev et al.,Nucl. Phys. A **229** (1997) 620.
[15] Ch. Egelhaaf et al., Nucl. Phys. A **405** (1983) 397.
[16] S.S. Rattan et al., J. Inorg. Nucl. Chem. **242** (1999) 551.
[17] S.Y.F. Chu et al., The Lund /LBNL Nuclear Data Search, 1999.
[18] N.A .Demekhina and G.S. Karapetyan, Phys. At. Nucl. **71** (2008) 27.
[19] I.V. Pokrovskij et al., Phys. Rev C **60** (1999) 041304.
[20] H. Kudo et al., Phys. Rev. C **57** (1998) 178.
[21] C.L. Brangaihno and V.J. Robinson, J. Inorg. Nucl. Chem. **39** (1977) 921.
[22] R.N. Sagaidak et al., Phys. Rev. C **68** (2003) 014603.
[23] S.S. Rattan et al., J. Radioanal. Nucl. **242** (1999) 551.
[24] S.E. Vigdor et al., Phys. Rev. C **26** (1982) 1035.
[25] S.S. Ratan et al., Radiochemica Acta **57** (1992) 7.
[26] M. Veselcky et al., Z. Phys. A **356** (1997) 403.
[27] Sh. A. Kalandarov et al., Phys. El. Part. Nucl. **43** (2012) 1591.
[28] Sh. A. Kalandarov et al., Phys. El. Part. Nucl. **26** (1982) 1035.
[29] D. Gardess et al., Phys. Rev. **18** (1978) 1298.
[30] S. Wild et al., Phys. Rev. C **32** (1985) 894.
[31] Y. Eyal et al., Phys. Rev. C **8** (1973) 1109.
[32] A. Gavron, Phys. Rev. C **21** (1980) 230.
[33] C. Birattari et al., Phys. Rev.C **54** (1996) 3051.
[34] E. Gadioli et al., Eur, Phys. J. A **11** (2001) 161.
[35] E. Gadioli et al., Nucl. Phys. A **708** (2002) 391.
[36] D.J. Fields et al., Phys.Rev. C **30** (1984) 1912.